(c)2001 American Institute of Aeronautics & Astronautics or Published with Permission of Author(s) and/or Author(s)' Sponsoring Organization.

A01-16102

AIAA 2001-0187

Microgravity Diode Laser Spectroscopy Measurements in a Reacting Vortex Ring

Shin-Juh Chen and Werner J.A. Dahm

Laboratory for Turbulence & Combustion (*LTC*)
Department of Aerospace Engineering
The University of Michigan
Ann Arbor, MI 48109-2140

Joel A. Silver

Southwest Sciences, Inc.
1570 Pacheco Street, Suite E-11
Santa Fe, NM 87505

Nancy D. Piltch

NASA-Glenn Research Center
M.S. 110-3
21000 Brookpark Road
Cleveland, OH 44153

39th AIAA Aerospace Sciences Meeting & Exhibit
8-11 January 2001 / Reno, NV

For permission to copy or republish, contact the American Institute of Aeronautics and Astronautics 1801 Alexander Bell Drive, Suite 500, Reston, VA 20191

(c)2001 American Institute of Aeronautics & Astronautics or Published with Permission of Author(s) and/or Author(s)' Sponsoring Organization.

Microgravity Diode Laser Spectroscopy Measurements in a Reacting Vortex Ring

Shin-Juh Chen[1] and Werner J.A. Dahm[2]

Laboratory for Turbulence & Combustion (LTC)
Department of Aerospace Engineering
The University of Michigan, Ann Arbor, MI 48109-2140

Joel A. Silver[3]

Southwest Sciences, Inc.
1570 Pacheco Street, Suite E-11
Santa Fe, NM 87505

Nancy D. Piltch[4]

NASA-Glenn Research Center
21000 Brookpark Road, M.S. 110-3
Cleveland, OH 44153

The technique of Diode Laser Spectroscopy (DLS) with wavelength modulation is utilized to measure the concentration of methane in reacting vortex rings under microgravity conditions. From the measured concentration of methane, other major species such as water, carbon dioxide, nitrogen, and oxygen can be easily computed under the assumption of equilibrium chemistry with the method of Iteractive Temperature with Assumed Chemistry (ITAC). The conserved scalar approach in modelling the coupling between fluid dynamics and combustion is utilized to represent the unknown variables in terms of the mixture fraction and scalar dissipation rate in conjunction with ITAC. Post-processing of the DLS measurements and the method of ITAC used in computing the species concentration are discussed. From the flame luminosity results, the increase in ring circulation appears to increase the fuel consumption rate inside the reacting vortex ring and the flame height for cases with similar fuel volumes. Preliminary results and application of ITAC show some potential capabilities of ITAC in DLS. The measured concentration of methane, and computed concentrations of water and carbon dioxide agree well with available results from numerical simulations.

1. INTRODUCTION

The field of Diode Laser Spectroscopy (DLS) with wavelength modulation [2,27] for species concentration measurements has advanced to the level where miniaturization of the laser and optical systems are possible for designing compact and rugged diagnostic systems with wide dynamic range and fast response time. This technique has been investigated previously by Silver *et al.* [29], and Silver & Kane [28] under microgravity condition for reacting flows. Measuring the species concentration of methane [13,20], water [14,23,29], carbon dioxide [21,25], carbon monoxide [20,24,31], hydroxyl radical [1] and molecular oxygen [22,24] are some of the possibilities of using diode lasers. In nonreacting flows without temperature variations, the measured species concentrations are trivially quantified using pre-determined calibration curves. However, for reacting flows, the determination of temperature is extremely important for the quantification of species concentrations from diode laser measurements. Often, a second laser is needed to work in pairs for determining the exact temperature field. This can be quite cumbersome due to space limitation and design constraints in monitoring systems. A generalized approach, referred herein as Iterative Temperature with Assumed Chemistry (*ITAC*), is suggested here. From the DLS measurements of a single major or minor species, the other remaining species can be determined with the assumption of equilibrium or non-equilibrium chemistry whichever appropriate for the flowfield been studied. The approach of a conserved scalar is taken here to model

1. Research Fellow; AIAA Member.
2. Professor; AIAA Senior Member; Corresponding author.
3. Vice president.
4. Research Scientist.

Copyright © by Shin-Juh Chen & Joel A. Silver

(c)2001 American Institute of Aeronautics & Astronautics or Published with Permission of Author(s) and/or Author(s)' Sponsoring Organization.

the interaction between fluid dynamics and combustion in reacting flows. This is the first time DLS system with the method of ITAC is used to probe flame-vortex interactions under microgravity conditions.

Flame-vortex interactions are canonical configurations that can be used to study the underlying processes occurring in complicated turbulent reacting flows. This type of configuration contains many of the fundamental aspects of the coupling between fluid dynamics and combustion that could be investigated with more controllable conditions than are possible under direct investigations of turbulent flames. The current configuration has been studied experimentally by Chen [4], Chen & Dahm [5–8], and Chen *et al.* [9–12] under microgravity conditions, and by Park & Shin [26], and You e*t al.* [32] under normal gravity conditions. This configuration is similar to that used in the analyses of Karagozian & Manda [16] and Manda & Karagozian [18] of their 2-D vortex pair in which both fuel and entrained oxidizer are present. The vortex ring used in this study is generated by issuing methane into an air environment through the exit of an axisymmetric nozzle. The experiments were conducted under microgravity conditions in order to remove the undesirable effects of buoyancy that can affect both the flame structure and ring dynamics resulting in possibly asymmetric and non-repeatable interactions [5].

Several key findings resulted from the numerical and experimental studies of this canonical configuration. Numerical simulations found that dilatation is the dominant effect of combustion heat release in a reacting vortex ring [11]. Effects of viscosity and mass diffusivity due to temperature on the flow, mixing, and combustion processes were found to be negligible in comparison to the effect of dilatation. For some of the ring circulation cases, the fuel consumption can be approximated by simple spherical diffusion estimates since the numerical simulations confirmed no presence of oxygen within the ring [10]. Furthermore, radiative heat loss was found to have an impact on the flame structure and ring dynamics of reacting vortex rings from comparison of cases of propane and ethane [10]. Concentration of major and minor species were determined from numerical simulation results of Chen *et al.* [9] and are yet to be verified

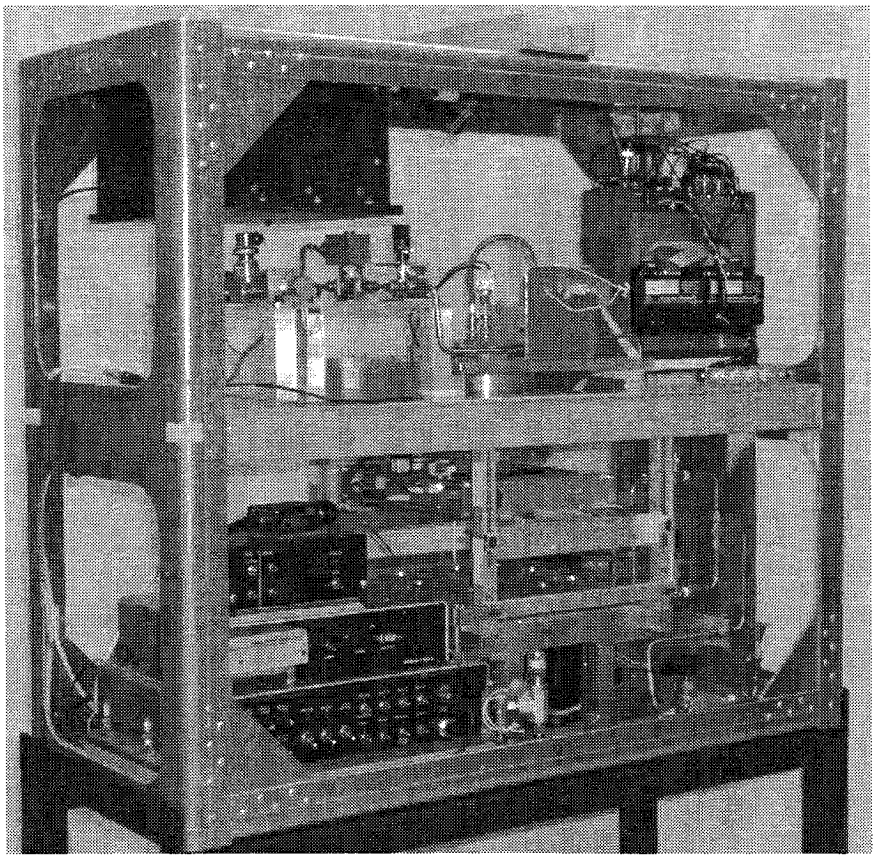

Figure 1. Experiment drop package showing vacuum system, power supply for spark generator, DLS controller and data acquisition system on top shelf. The vortex generator system, power distributor, batteries, B/W CCD camera, test section, nozzle/plenum assembly and video transmitters reside on the bottom shelf.

(c)2001 American Institute of Aeronautics & Astronautics or Published with Permission of Author(s) and/or Author(s)' Sponsoring Organization.

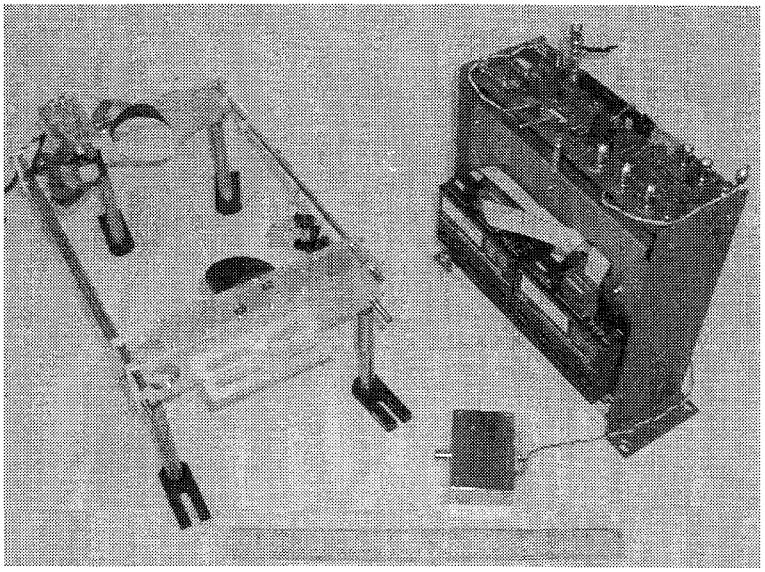

Figure 2. Compact and rugged DLS system showing the laser setup (*left*); DSP board, controller and data acquisition box (*right*); and pre-amplifier box (*middle*).

experimentally.

DLS is used to measure the concentration of methane for reacting vortex rings under microgravity conditions. The experiment drop package along with the DLS system is discussed. The processing and post-processing of measured spectra and the determination of species concentration from the spectra using ITAC are also presented. Preliminary DLS/ITAC measurements are compared to the numerical simulations of Chen *et al.* [10].

2. EXPERIMENT METHODS

2.1. Microgravity Drop Rig

Figure 1 shows the experiment drop rig with an integrated DLS system (see Fig. 2). The rig has been previously used for microgravity experiments at the NASA-Glenn 2.2 seconds drop tower facility by [4–12]. This is a 24.1 m tower where experiment is loaded unto a drag shield, for the reduction of air resistance during the free-fall, on the 5th floor, released from the 8th floor, and lands on an inflated airbag in the basement floor. The experiment rig is then retrieved from the basement floor to the 5th floor for data collection and preparation for additional drops.

For studying lighter-than-air fuels, the nozzle/plenum assembly is pointing downward. This is a matter of convenience since under normal gravity condition this is the most stable position for keeping methane inside the nozzle/plenum assembly. The top shelf houses a vacuum system, DLS controller and data acquisition box, DLS power distributor, and spark power supply. The bottom shelf houses the nozzle/plenum assembly, test section, DLS laser system and pre-amplifier box, vortex generator system, power distributor, video transmitter, batteries, and B/W CCD camera. The camera records the flame structure and ring dynamics of reacting vortex rings. Details of the hardware for the microgravity drop rig are discussed in Chen [4].

Prior to each microgravity experiment, the vortex generator and nozzle/plenum systems are purged with fuel. Pressurized fuel (30-80 psig) is stored in one section of the fluid system. The test section is open to the atmosphere and is purged with air to remove dust particles. A motor-driven iris diaphragm remains closed to separate the fuel and air interfaces near the nozzle exit (D = 2 cm dia.).

Prior to a microgravity drop, the nozzle/plenum is repurged with fuel to remove air that has diffused through the iris leaves and opening. Once all the systems have been turned on including the DLS system, the iris diaphragm opens to allow inter-diffusion between the fuel and air interfaces. A diffusion layer is formed and drawn towards an ignitor, which lies inside the nozzle/plenum assembly, by suction from a vacuum system. The experiment rig is released from the ceiling of the 8th floor and ignition occurs 50-60 ms after the drop. A diffusion flame is generated near the nozzle exit and flattens under microgravity conditions. Pressurized fuel is released into the nozzle/plenum assembly and issues out of the nozzle to generate a vortex ring which wraps the diffusion flame to generate a reacting vortex ring. Flame luminosity is recorded unto s-VHS tape by the on-board CCD camera for later analysis. Video signals

(c)2001 American Institute of Aeronautics & Astronautics or Published with Permission of Author(s) and/or Author(s)' Sponsoring Organization.

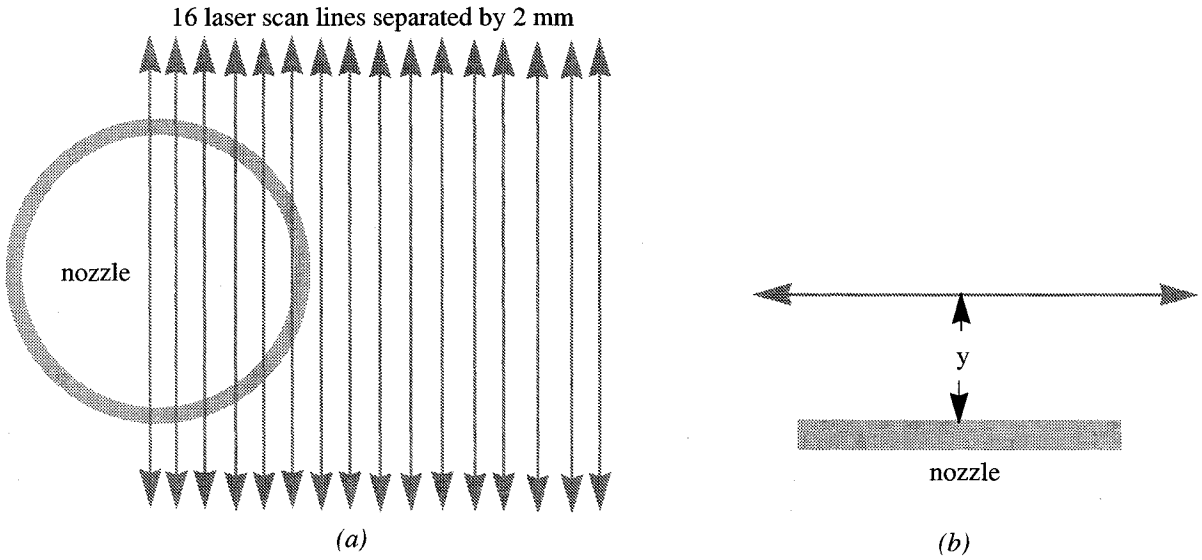

Figure 3. Schematic showing the position of the 16 laser scan lines used in the laser system. *(a)* Top view shows the scan lines spanning 30 mm from the center of the 2-cm diameter nozzle. *(b)* Side view of the scan lines showing the height of the lines relative to the nozzle exit plane.

are sent from the CCD camera to recording station on the 8th floor using fiber optic cables.

2.2. DLS System

Figure 2 shows the DLS system which includes the laser system, digital signal processor (DSP) board, controller and data acquisition system, and pre-amplifier box. The laser beam is collimated by an anti-reflection coated aspheric lens and is pointed onto a raster scanner mirror. As the mirror is rotated over an angle of about 30°, the reflected laser beam hits an off-axis paraboloidal reflector (OAP). The scanner mirror is positioned at the focus of this OAP so that all rays reflected by the OAP are parallel. As the beam is swept by the scanner, it tracks in parallel lines across the flame. After traversing the flame, a second off-axis paraboloid collects the beam and refocuses it onto a single photodetector. This optical system can scan a range of up to 4 cm. The result of this process is that data acquired sequentially in time are used to obtain spatially-resolved line-of-sight measurements across the flame. More details on this approach can be found in Silver & Kane [28].

Wavelength modulation spectroscopy (WMS) detection is accomplished by digitally modulating the laser wavelength at 25 kHz and detecting the $2f$ (50 kHz) component of the photocurrent. A modified square wave modulation waveform is used [15]. Data are recorded using the analog inputs to a stand-alone DSP supercontroller. This device generates the scanner and laser ramp/modulation waveforms, acquires and processes all data, and stores the data to memory for subsequent download to a laptop computer after the drop is completed. The DSP board is housed in a small electronics box mounted on the top shelf of the drop rig. This box also contains the laser and scanner controllers, and the necessary cable interfaces.

This system is anticipated to detect CH_4, O_2, CO_2, H_2O, and OH. For the detection of oxygen at 760 nm (visible), a GaAlAs vertical cavity surface emitting laser can be used. The other gases can be detected using near-infrared InGaAsP distributed feedback lasers at the specific wavelengths required for each gas. In this experiment methane detection is achieved using a 1653.5 nm laser.

Before the drop the system stores data in a circular buffer, so as to have pre-drop spectra if necessary and to aid in setting up the proper operating conditions. Upon receiving the drop trigger (using an accelerometer), the most recently acquired pre-drop data (spatially-mapped spectra) is stored, and then sequential data blocks corresponding to approximately 100 msec periods are acquired, demodulated, processed and stored. After the drop, the data is downloaded via a serial port to a laptop computer for subsequent analyses.

One advantage of the modified square wave WMS approach is that it requires only one cycle of the waveform at each wavelength, so that scanning can be accomplished quite rapidly. Using the 200 kHz digitizer, the laser wavelength is incremented at 50 kHz (4 steps/waveform). With a spectrum length of 125 points, this system is capable of measuring 40 spatial locations at 10 Hz.

(c)2001 American Institute of Aeronautics & Astronautics or Published with Permission of Author(s) and/or Author(s)' Sponsoring Organization.

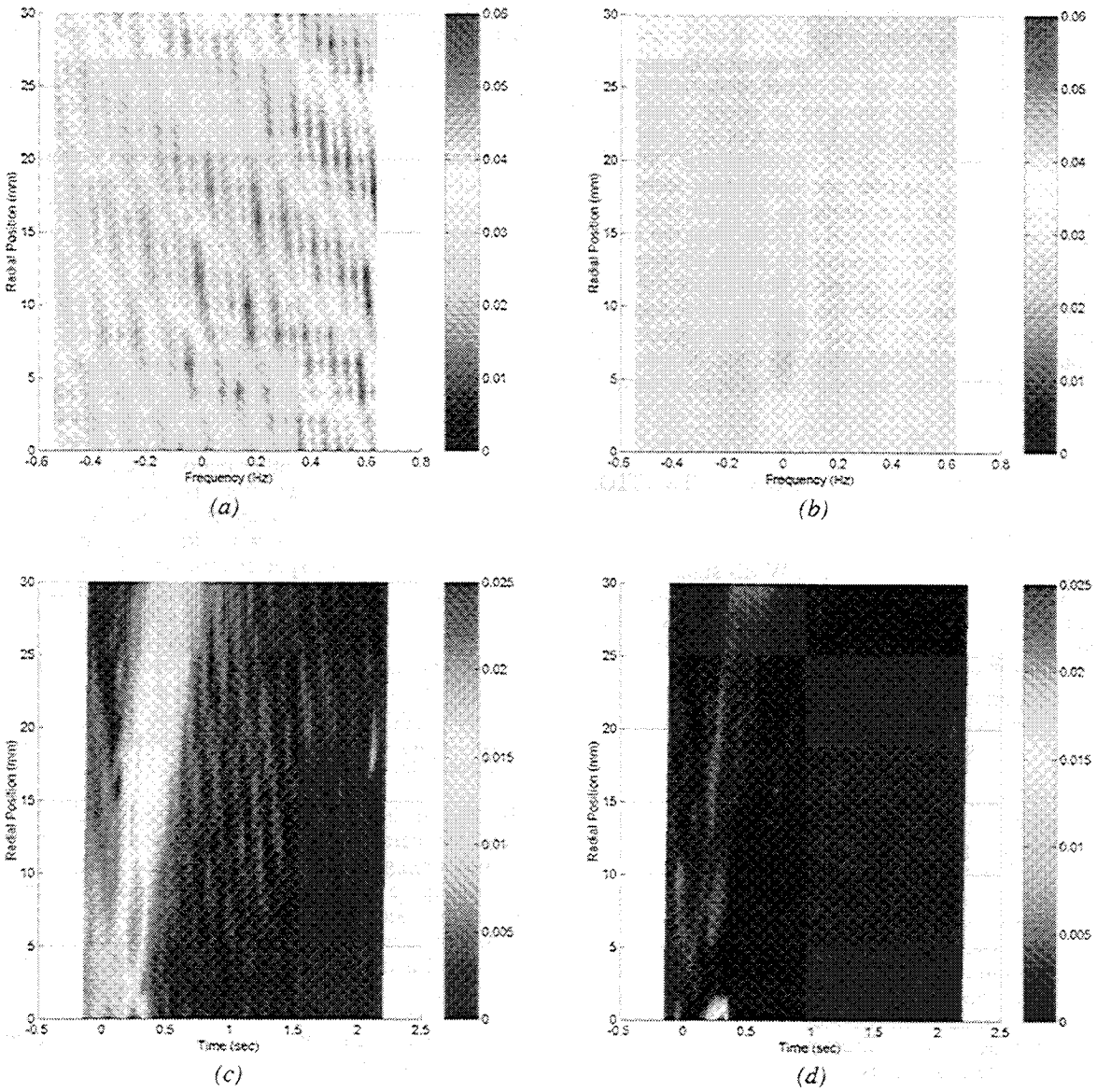

Figure 4. Sample spectra and absorbances for a nonreacting vortex ring as a result of issuing methane into an air environment at atmospheric conditions at y = 6.35 mm under microgravity. *(a)* Unfiltered absorbance spectra containing étalons for time 0.160 s, *(b)* absorbance spectra with étalons successfully filtered out for time 0.160 s, *(c)* projection absorbance, *(d)* Abel-inverted radial absorbance.

For the current experiments, Fig. 3a shows the system is set to sample over 16 horizontal locations separated by 2 mm at a rate of 20 Hz spanning 30 mm outward from the center of the nozzle. Figure 3b shows the vertical positioning of the scanning system relative to the nozzle exit plane and can be set to any desired height y.

3. POST-PROCESSING SPECTRA

The measured spectra from DLS were filtered to remove unwanted étalons that were present in all the measurements. With properly chosen filters, the étalons present in Fig. 4a can be effectively removed to generate étalon-free results as shown in Fig. 4b. The presence of étalons does compromise the sensitivity of the DLS system, however, since high concentrations of methane are of interest, such compromise is of no concern. The étalons can be removed with better optimization of the optical system to achieve better sensitivity.

Post-drop processing of the filtered spectra comprises least squares fitting to reference spectra. The data are fit

(c)2001 American Institute of Aeronautics & Astronautics or Published with Permission of Author(s) and/or Author(s)' Sponsoring Organization.

to a function composed of a theoretical line shape plus background polynomial term giving Fig. 4c. A multi-linear regression method has proven to be rapid and accurate. For flames that are axisymmetric as is the case in these reacting vortex rings, an Abel inversion is invoked to obtain radial concentration profiles as shown in Fig. 4d. Calibration for all of the permanent gases is easily accomplished in room air or using a calibration cell. The system calibration function is very stable and can be used without frequent recalibrations. For OH, one will probably transfer the calibration from water vapor, using relative line strengths of these gases. Gas concentrations are determined directly from the absorption data. Local gas temperature can be inferred from either O_2 line pairs, or possibly lines in the OH band head near 1393 nm. However, a different technique in obtaining local temperatures, which are necessary for computing accurate mole fraction of the measured gas concentrations, is proposed here and discussed next.

4. COMPUTING SPECIES CONCENTRATION

4.1. Background

The process of converting radial WMS signals to mole fraction can be done in several ways. The problem is trivial for nonreacting flows since there exists relations to convert radial absorbance from DLS to mole fraction. In reacting flow, the fundamental problem is that one needs temperature field in order to obtain concentration field. One technique involves choosing an absorption line with a cross-section-to-temperature ratio that varies negligibly with temperature for the range of temperature to be explored. The second technique determines the temperature from the ratio of two absorption lines that have different ground-state energies. The third technique requires fitting WMS line shape to extract local temperature. This technique only works if the line shapes are sensitive to temperature. The fourth technique employs numerical simulations to obtain a reasonable temperature field of the reacting flow field from which quantitative measurements of combustion species can be computed from the recorded WMS signals. A fifth technique involves direct measurements of temperature using thermocouples.

Here a new technique to determine temperature field from the WMS signals to facilitate the computation of species concentration is proposed. This new idea extends a single measurement of major or minor species to include all other major or minor species to be derived from a single measurement.

The conserved scalar approach in modelling the coupling between fluid dynamics and combustion can only represent small departures from chemical equilibrium. This approach can be broken down into several types depending on the chemistry assumption. These are equilibrium chemistry, flamelet (non-equilibrium chemistry), Conditional Moment Closure (CMC), and Strained Diffusion Reaction Layer (SDRL). Here, the focus is on equilibrium and non-equilibrium chemistry. The conserved scalar approach reduces the number of unknowns to one (ζ) or two (ζ, χ) depending on the chemistry assumption, where ζ denotes the mixture fraction, and χ the scalar dissipation rate.

The proposed idea in determining the temperature field from the measured WMS signals include an iterative process (ITAC) in which chemistry assumptions play an important role. In an axisymmetric flow configuration, such as the case of a reacting vortex ring, radial profile of absorbance are available after Abel inversions of line-of-sight measurements. The procedures in obtaining species mole fractions from radial absorbance are outlined below for different choices of chemistry assumption.

4.2. Equilibrium Chemistry

In the case of equilibrium chemistry, temperature and major species concentration are uniquely determined from the mixture fraction. From the measurement of a major chemical species (e.g. CH_4, O_2, CO_2, or H_2O), one can determine the other major species and temperature field. Temperature field is critical for obtaining concentrations of major species from the WMS signals. Instead of having two unknowns, which are temperature and a major species mole fraction, there is only one unknown (the mixture fraction ζ) which needs to be determined. The value of ζ ranges from 0 (no fuel) to 1 (pure fuel). Note that non-adiabatic effects are not considered here, such as heat losses from the nozzle. For regions where the measured concentration of a major species is zero or below the sensitivity of the system, determining the other major species and temperature is not possible.

For the methane-air combustion, a table of major species, temperature, and mixture fraction is composed from running CET93 [19] for several mixture conditions. Figure 5 shows the temperature and concentration of major species variation with mixture fraction. The peak temperature of 2226 K is around the stoichiometric mixture fraction ζ_s of 0.055 and concentration of water is found throughout the mixture fraction space. Carbon dioxide is found from $\zeta = 0$ to 0.55. However no methane is found near the stoichiometric point and on the fuel-lean side as well.

At each spatial location, DLS measurements of methane mole fraction is provided at an arbitrary temperature of 296 K. The following procedures are used to correct the DLS measurements.

- Guess the mixture fraction. The corresponding mixture fraction for the initial mole fraction as read from equilibrium chemistry tables can be used as the initial guess.
- Obtain mole fraction of CH_4 and temperature for the guessed mixture fraction using the composed equilibrium chemistry from CET93.
- Correct mole fraction of CH_4 (initially at 296 K) from WMS signals using the temperature obtained from second step and multiplying the mole fraction by a temperature-dependent factor *f*. The mole fraction of methane changes at each temperature

(c)2001 American Institute of Aeronautics & Astronautics or Published with Permission of Author(s) and/or Author(s)' Sponsoring Organization.

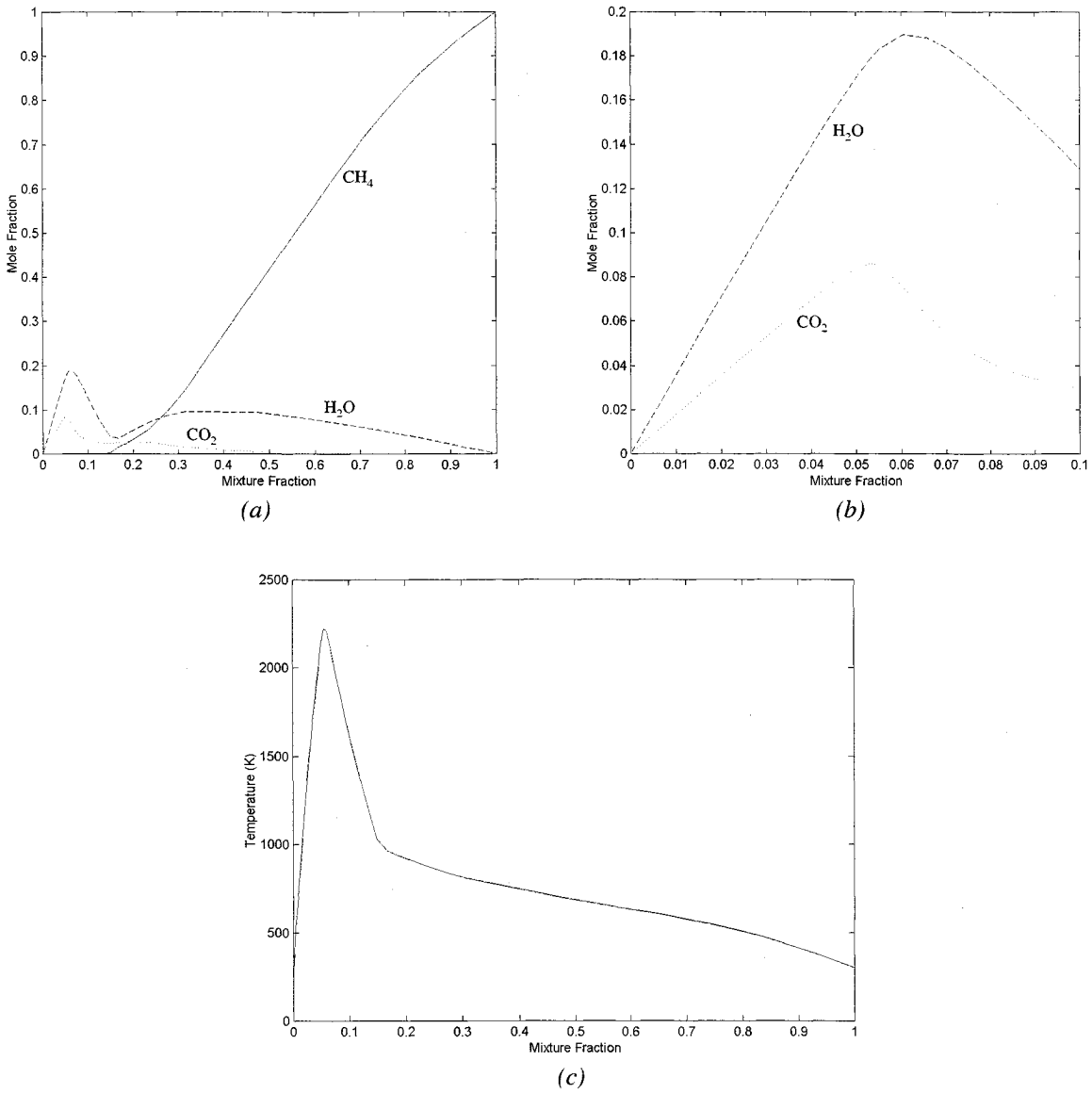

Figure 5. Equilibrium chemistry state relations for methane-air reaction using CET93 [19]. *(a)* Mole fractions of CH_4, CO_2, and H_2O as function of mixture fraction with a close-up region shown in *(b)*. *(c)* Temperature variation with mixture fraction for adiabatic conditions.

due to decrease in number density and absorption cross section.

- Compare the mole fraction obtained from the equilibrium chemistry with that obtained from the WMS signals. If the two values are comparable, then the correct temperature was obtained. If not, then the above procedures are repeated.

$$f = a_0 - a_1 T + a_2 T^2 - a_3 T^3 + a_4 T^4,$$

where T denotes the local temperature in Kelvin, and the coefficients are a_0 = 0.67431, a_1 = 0.001875, a_2 = 1.1451e^{-5}, a_3 = 4.8148e^{-9}, and a_4 = 3.6881e^{-12}.

This technique is applied to DLS measurements of CH_4 concentration in a reacting vortex ring under microgravity conditions, and the results are discussed in §5.

4.3. Non-Equilibrium Chemistry

When the diffusive time scale is larger than the chemical time scale, non-equilibrium chemistry assumption is

(c)2001 American Institute of Aeronautics & Astronautics or Published with Permission of Author(s) and/or Author(s)' Sponsoring Organization.

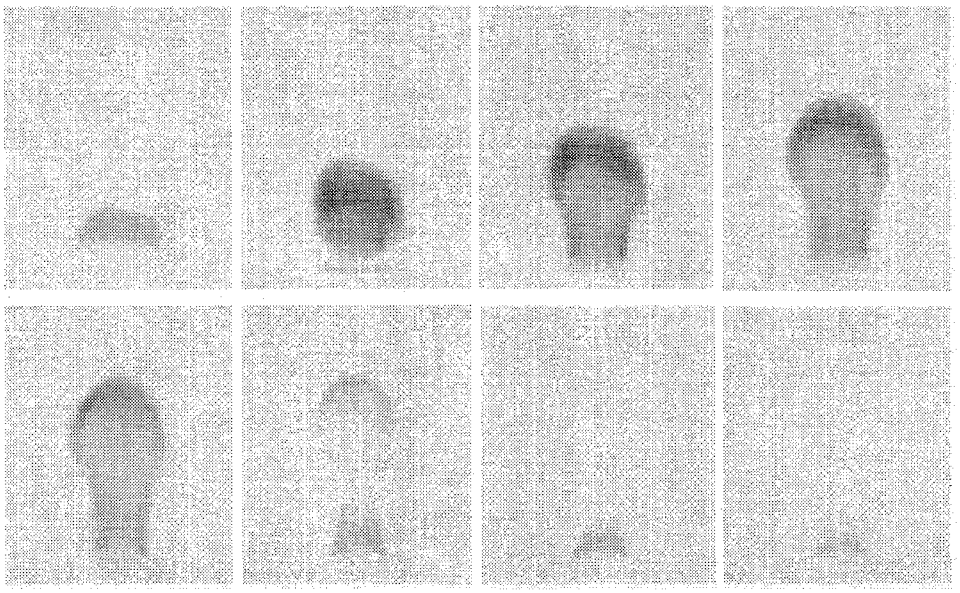

Figure 6. Flame luminosity results showing methane-air combustion for ring circulation of 482 cm^2/s and fuel volume of 22 cc under microgravity conditions.

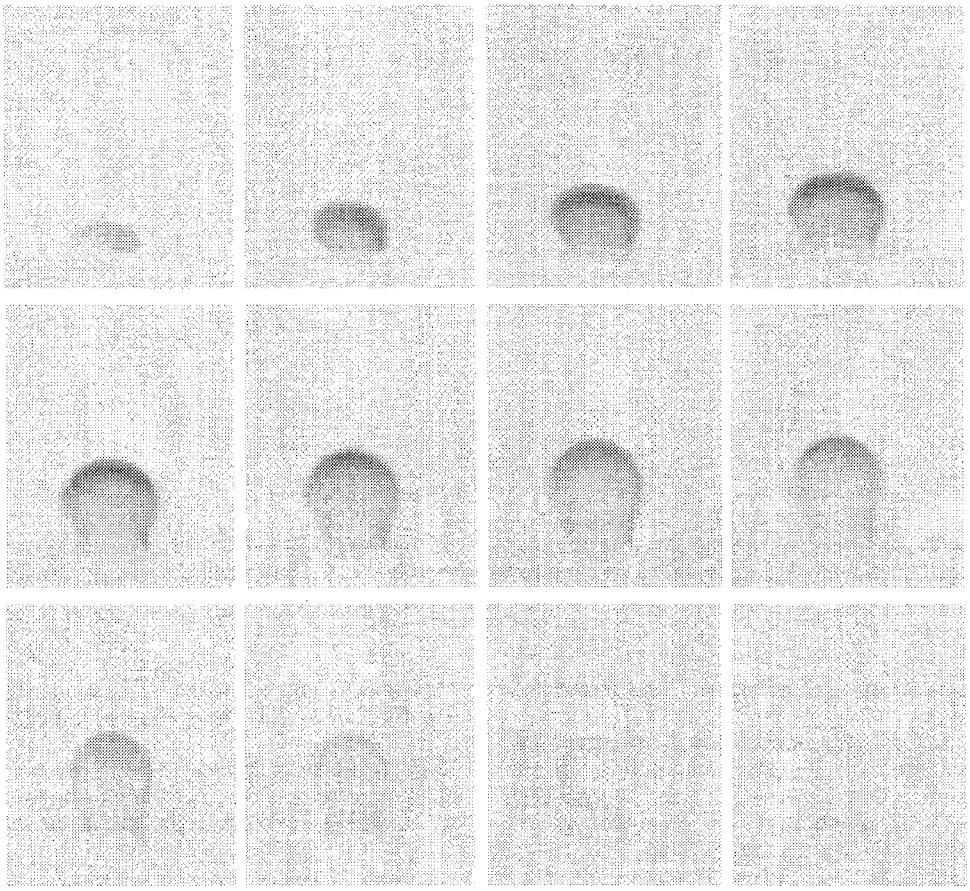

Figure 7. Flame luminosity results showing methane-air combustion for ring circulation of 212 cm^2/s and fuel volume of 21 cc under microgravity conditions.

(c)2001 American Institute of Aeronautics & Astronautics or Published with Permission of Author(s) and/or Author(s)' Sponsoring Organization.

more appropriate especially for the computation of minor species. In such situation, the temperature and species concentration are functions of mixture fraction and scalar dissipation rate (ζ, χ). Mixing and chemistry processes occurring within the flame can be locally approximated by an opposed-flow diffusion flame configuration where reaction occurs in thin regions. The scalar dissipation rate sets the molecular mixing rate between the fuel and oxidizer.

The OPPDIF code [17] with GRI-Mech 2.11 kinetics [3] is utilized to build a table of temperature and species concentrations as functions of (ζ, χ). DLS measurements of a major species (e.g. CH_4) and a minor species (e.g. OH) concentrations are necessary for the correct determination of the local temperature. Iterations will proceed by choosing an initial pair of (ζ, χ) and updating the pair until the correct temperature is obtained. Thus the quantitative measurements of all the major and minor species can be determined from the correct pair of (ζ, χ) and the corresponding local temperature. This technique will be applied to future DLS measurements of OH concentration in reacting vortex rings in addition to CH_4 measurements.

5. RESULTS AND DISCUSSIONS

5.1. Flame Luminosity Results

Video images of flame luminosity from a B/W CCD camera reveal the flame structure and dynamics of reacting vortex rings under microgravity conditions. Figures 6 & 7 shows reacting vortex rings generated from issuing methane out of the circular nozzle with a diffusion flame already established at the nozzle exit. As the ring forms, it wraps the diffusion layer and travels downstream while consuming the fuel. Both cases have similar fuel volume V_F but different ring circulations Γ. Case A has $\Gamma = 482$ cm^2/s and $V_F = 22$ cc. Case B has $\Gamma = 212$ cm^2/s and $V_F = 21$ cc. Radiative heat loss due to the presence of soot can be neglected since dark regions are not prevalent in the images. These dark regions are usually indication of the presence of soot [12]. However radiative heat losses from CO_2 and H_2O are still present in these methane-air burning rings.

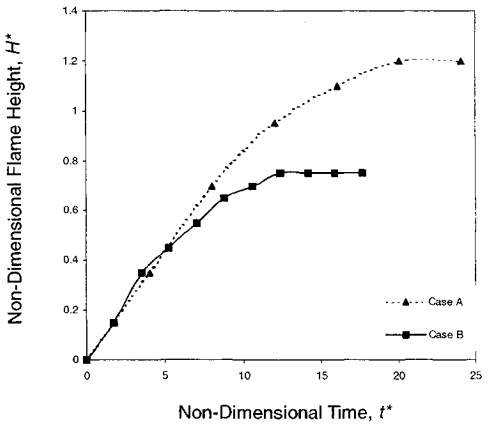

Figure 8. Methane-air results for the effect of ring circulation on ring trajectory $H^*(t^*)$ with similar fuel volumes. Ring circulations are 482 and 212 cm^2/s for Case A and B, respectively.

The effect of ring circulation on the flame structure and ring dynamics can be clearly observed. It is obvious that since case A has higher ring circulation it will travel further downstream as shown in Fig. 6. The visible flame height is denoted by H. In addition, there is an enhancement in the consumption of fuel by the reaction due to the increase in ring circulation. When plotted on non-dimensional variables of $H^* = H/D$ and $t^* = t\Gamma/D^2$ as shown in Fig. 8 the ring trajectories should collapse to a single curve for nonreacting vortex rings with the assumption of similar core structures. However, in reacting vortex rings, dilatation can greatly affect the ring trajectories [10]. No increase in dilatation was observed for rings with ring circulations lower than 200 cm^2/s. However, one should expect an increase in dilatation due to an increase in mixedness as a result of increased ring circulation [30]. With an increased mixedness, there should be a noticeable increase in the ring trajectory due to increased dilatation. For the range of ring circulation studied here (200-500 cm^2/s), the increase in ring circulation has indeed contributed to an increase in fuel consumption rate which promoted an increase in flame height due to increased dilatation.

5.2. Species Concentration and Temperature Field

The conditions of Case B were chosen to demonstrate the method of ITAC with DLS measurements of methane. The laser scan lines were positioned 6.35 mm above the nozzle exit plane and spanned 30 mm horizontally. Figure 9 shows the temporal and spatial variation of methane mole fraction for uncorrected and corrected values. The correction of the methane mole fraction can only be accomplished by accurately knowing the local temperature. Methane is still present along the 30 mm scan line which indicates that the scanning region has not completely enclosed the burning vortex ring. Future measurements may need to extend the scanned regions further outward (40 mm) from the nozzle center to visualize the complete burning vortex ring. Although the regions near the centerline ($r = 0$) do not show the correct methane concentration field, much can be gained by applying ITAC to the current measurements. Preliminary results are used as demonstrations of this methodology which was explained in §4.

From the DLS measurements of radial absorbance after post-processing of spectra as demonstrated earlier in Fig. 4, methane mole fraction (see Fig. 9a) can be computed with the assumption of a temperature field (e.g. 296 K) using calibration curves. The temperature field needs to be determined in order to obtain the correct mole fraction of methane. The method of ITAC outlined earlier with the assumption of equilibrium chemis-

(c)2001 American Institute of Aeronautics & Astronautics or Published with Permission of Author(s) and/or Author(s)' Sponsoring Organization.

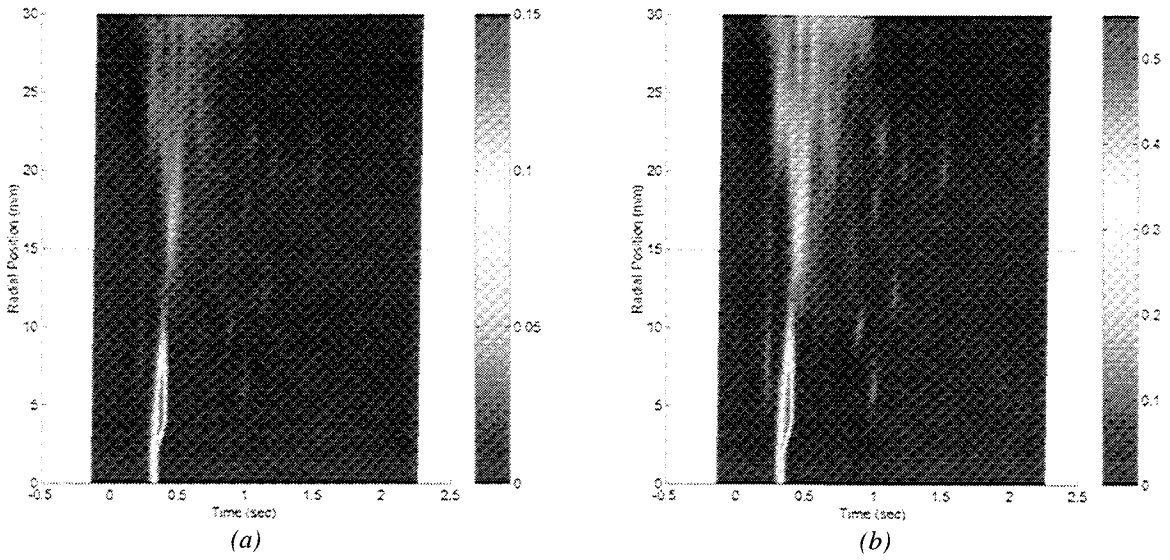

Figure 9. Reacting vortex ring results showing temporal and spatial evolution of CH_4 mole fraction at y = 6.35 mm under microgravity conditions. *(a)* Uncorrected concentration using an assumed temperature of 296 K, *(b)* corrected concentration using a temperature field determined from ITAC.

try can be used to provide the correct temperature by first determining the correct mixture fraction field. Instead of solving for two unknowns (T and CH_4 mole fraction), one only needs to solve for one single variable, namely the mixture fraction ζ. With the mixture fraction determined, the major species and temperature can be easily obtained from state relationships for equilibrium chemistry as shown in Fig. 5.

This iterative procedure guesses the mixture fraction field which then gives a corresponding temperature field and molar concentration of methane by referring to state relationships for equilibrium chemistry (Fig. 5). The temperature field is used to update the molar concentration of methane obtained from DLS measurements. The molar concentrations of methane obtained from DLS and ITAC are compared, and if there is a close match then the correct temperature has been determined. This iterative procedure is applied to all DLS data points. The final molar concentration field of methane is shown in Fig. 9b with the corresponding mixture fraction and temperature field shown in Figs. 10a and 10b, respectively. In regions where molar concentration of methane is zero or below the sensitivity of the system, the mixture fraction and temperature cannot be determined. DLS measurements of CO_2 and H_2O may be a better choice since their concentrations span the whole spectrum of mixture fraction shown in Fig. 5.

With the mixture fraction determined, obtaining the mole fraction of the other major species such as CO_2 and H_2O can be trivially done using the state relationships established in Fig. 5 with equilibrium chemistry. CO_2 mole fraction is shown in Fig. 10c. Large concentrations of CO_2 appears in the latter stage of interaction and away from the nozzle (> 10 mm). High concentration of CO_2 are found in regions where the fuel has been consumed by the reaction.

As for the H_2O mole fraction (see Fig. 10d), H_2O appears to be present even in regions where there is still fuel to be consumed by the reaction. High concentration of H_2O appears in the early stage and extends from the nozzle center and outward, contrary to CO_2 concentration fields. The results of CO_2 and H_2O mole fraction are consistent with the numerical simulation results of Chen *et al.* [10].

6. CONCLUSIONS

Diode laser spectroscopy measurements with the method of Iterative Temperature with Assumed Chemistry was successfully implemented in the study of reacting vortex rings under microgravity conditions. This method eliminates the need to solve for two unknowns (T, CH_4 mole fraction) by finding the appropriate mixture fraction field for equilibrium chemistry assumption. Once the correct mixture fraction field is determined, all the major species and temperature are easily determined from interpolating tables. With the measurement of a single major species such as methane, this method can be applied to find the correct temperature field and all the other major species without having to conduct additional experiments or install additional lasers. The method of ITAC extends diode laser spec-

(c)2001 American Institute of Aeronautics & Astronautics or Published with Permission of Author(s) and/or Author(s)' Sponsoring Organization.

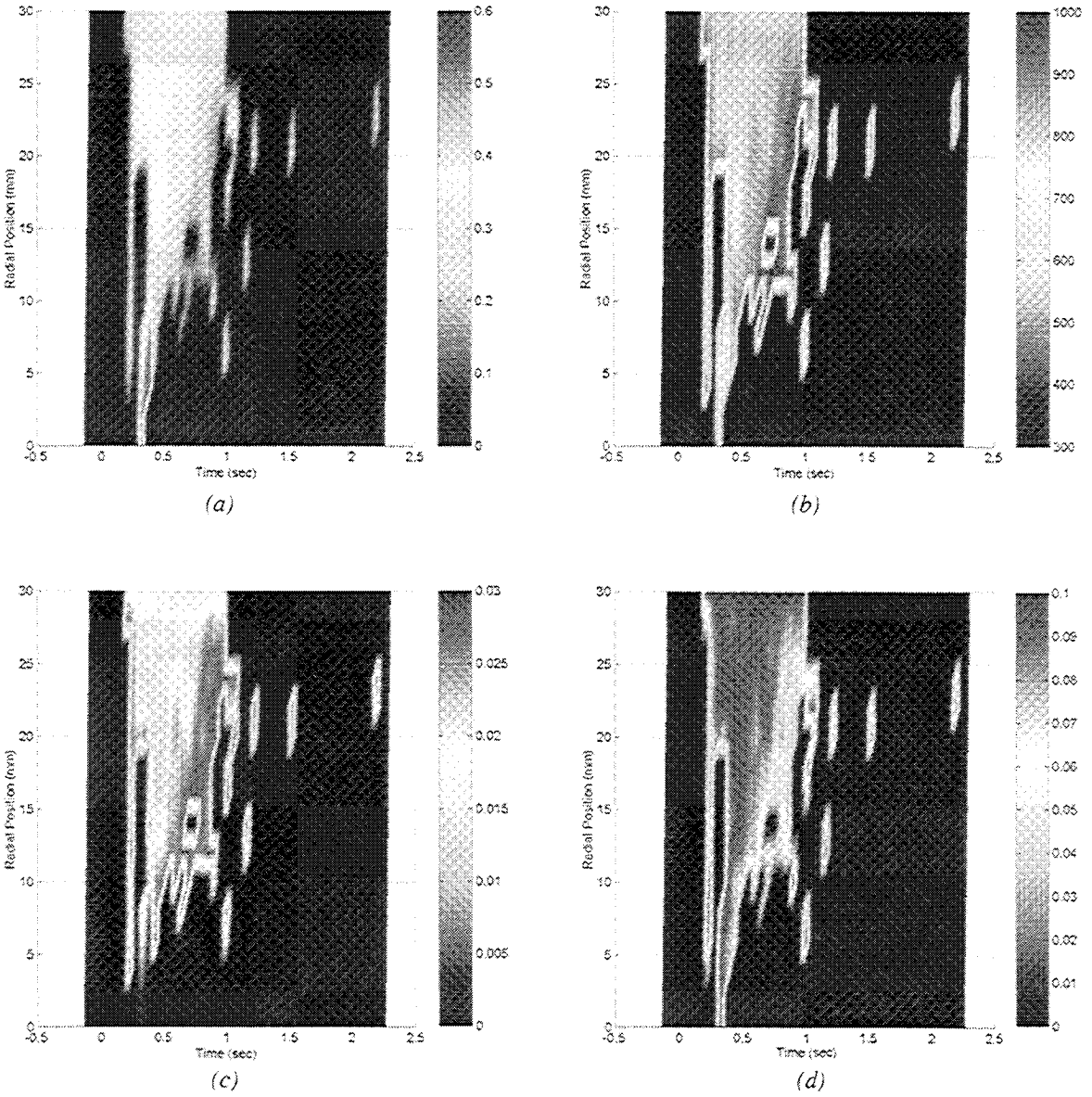

Figure 10. Reacting vortex ring results showing temporal and spatial evolution of *(a)* mixture fraction, *(b)* temperature in K, *(c)* CO_2 mole fraction, and *(d)* H_2O mole fraction at y = 6.35 mm under microgravity conditions, as a result of applying ITAC to initial DLS measurements of CH_4 mole fraction which were computed at 296 K.

troscopy measurement technique of a single species to a much broader measurement technique.

Flame luminosity results have identified the effect of ring circulation on the flame structure and ring dynamics. The increase in ring circulation with similar fuel volume has contributed to an increase in fuel consumption rate inside the vortex ring and an increase in flame height. The measured concentrations of CH_4, and computed H_2O and CO_2 agree well with the numerical simulations results of Chen *et al.* [10] at least for the regions away from the centerline ($r = 0$).

Further experiments will include a detailed probing of the reacting vortex rings at several heights from the nozzle exit plane under microgravity conditions with DLS measurements of CH_4 and OH and possibly H_2O. In addition, the method of Iterative Temperature with Assumed Chemistry will be applied with the assumption of non-equilibrium chemistry in later studies.

(c)2001 American Institute of Aeronautics & Astronautics or Published with Permission of Author(s) and/or Author(s)' Sponsoring Organization.

Acknowledgements

This research is been sponsored by the NASA Microgravity Combustion Science Program under Contract No. NASA-G-NAG3-1639 at the University of Michigan, and under Contract No. NASA-NAS3-99140 at Southwest Sciences, Inc.

References

[1] Aizawa, T., Kamimoto, T., and Tamaru, T. (1999) Measurements of OH radical concentration in combustion environments by wavelength-modulation spectroscopy with a 1.55 μm distributed-feedback diode laser. *Appl. Opt.* **38** (9):1733-1741.

[2] Bomse, D.S., Stanton, A.C., and Silver, J.A. (1992) Frequency modulation and wavelength modulation spectroscopies: comparison of experimental methods using a lead-salt diode laser. *Appl. Opt.* **31**:718.

[3] Bowman, C.T., Hanson, R.K., Davidson, D.F., Gardiner, W.C. Jr., Lissianski, V., Smith, G.P., Golden, D.M., Frenklach, M., and Goldenberg, M. GRI-mech 2.11, *http://www.me.berkeley.edu/gri-mech/*.

[4] Chen, S.-J. (2000) Experimental and computational study of fluid dynamics-combustion coupling in a diffusion flame-vortex ring interaction. *Ph.D. dissertation*. University of Michigan, Ann Arbor, Michigan.

[5] Chen, S.-J., and Dahm, W.J.A. (1997) Vortex ring/diffusion flame interactions in microgravity conditions. *Fourth International Microgravity Combustion Workshop*, NASA CP-10191, 191-196.

[6] Chen, S.-J., and Dahm, W.J.A. (1998) Diffusion flame structure of a laminar vortex ring under microgravity conditions. *Proc. Combust. Inst.* **27**:2579-2586.

[7] Chen, S.-J., and Dahm, W.J.A. (1999) Experiments on diffusion flame structure of a laminar vortex ring. *First Joint Meeting of the U.S. Sections of the Combustion Institute*, The Combustion Institute, Pittsburgh, PA, 461-464.

[8] Chen, S.-J., and Dahm, W.J.A. (1999) The interaction of a vortex ring with a diffusion flame under microgravity conditions. *Fifth International Microgravity Combustion Workshop*, NASA CP-208917, 271-274.

[9] Chen, S.-J., Dahm, W.J.A., and Tryggvason, G. (2000) Coupling between fluid dynamics and combustion in a laminar vortex ring. *AIAA Paper No. 2000-0433*, AIAA, Washington, DC.

[10] Chen, S.-J., Dahm, W.J.A., and Tryggvason, G. (2000) Results from numerical simulations of the diffusion flame-vortex ring interaction. *AIAA Paper No.* 2000-2468, AIAA, Washington, DC.

[11] Chen, S.-J., Dahm, W.J.A., and Tryggvason, G. (2000) Effects of heat release in a reacting vortex ring. *Proc. Combust. Inst.* **28**. To Appear.

[12] Chen, S.-J, Dahm, W.J.A., Millard, M., and Vander Wal, R.L. (2001) Laser soot-mie scattering in a reacting vortex ring. *AIAA Paper No.* 2001-0786.

[13] Chou, S.-I., Baer, D.S., and Hanson, R.K. (1997) Diode laser absorption measurements of CH_3Cl and CH_4 near 1.65 μm. *Appl. Opt.* **36** (15):3288-3293.

[14] Hovde, D.C., and Parsons, C.A. (1997) Wavelength modulation detection of water vapor with a vertical cavity surface-emitting laser. *Appl. Opt.* **36** (6):1135-1138.

[15] Iguchi, T. (1986) Modulation waveforms for second harmonic detection with tunable diode lasers. *J. Opt. Soc. Am.* **B 3**:419-423.

[16] Karagozian, A.R., and Manda, B.V.S. (1986) Flame structure and fuel consumption in the field of a vortex pair. *Combust. Sci. Tech.* **49**:185-200.

[17] Kee, R.J., Rupley, F.M., Miller, J.A., Coltrin, M.E., Grcar, J.F., Meeks, E., Moffat, H.K., Lutz, A.E., Dixon-Lewis, G., Smooke, M.D., Warnatz, J., Evans, G.H., Larson, R.S., Mitchell, R.E., Petzold, L.R., Reynolds, W.C., Caracotsios, M., Stewart, W.E., and Glarborg, P. (1999) *CHEMKIN Collection*, Release 3.5, Reaction Design, Inc., San Diego, CA.

[18] Manda, B.V.S., and Karagozian, A.R. (1988) Effects of heat release on diffusion flame-vortex pair interactions. *Combust. Sci. Tech.* **61**:101-119.

[19] McBride, B.J., Reno, M.A., and Gordon, S. (1994) CET93 and CETPC: An interim updated version of the NASA Lewis Computer program for calculating complex chemical equilibria with applications. *NASA Tech. Mem.* 4557.

[20] Mihalcea, R.M., Baer, D.S., and Hanson, R.K. (1997). Diode laser sensor for measurements of CO, CO_2, and CH_4 in combustion flows. *Appl. Opt.* **36** (33):8745-8752.

[21] Mihalcea, R.M., Baer, D.S., and Hanson, R.K. (1998) Diode-laser absorption measurements of CO_2 near 2.0 μm at elevated temperatures. *Appl. Opt.* **37** (36):8341-8347.

[22] Miller, M.F., Kessler, W.J., and Allen, M.G. (1996) Diode laser-based air mas flux sensor for subsonic aeropropulsion inlets. *Appl. Opt.* **35**:4905-4912.

[23] Nagali, V., and Hanson, R.K. (1997) Design of a diode-laser sensor to monitor water vapor in high-pressure combustion gases. *Appl. Opt.* **36** (36):9518-9527.

[24] Nguyen, Q.V., Dibble, R.W., and Day, T. (1994)

(c)2001 American Institute of Aeronautics & Astronautics or Published with Permission of Author(s) and/or Author(s)' Sponsoring Organization.

High-resolution oxygen absorption spectrum obtained with an external-cavity continuously tunable diode lasers. *Opt. Lett.* **19**:2134-2136.

[25] Oh, D.B., Paige, M.E., and Bomse, D.S. (1998) Frequency modulation multiplexing for simultaneous detection of multiple gases by use of wavelength modulation spectroscopy with diode lasers. *Appl. Opt.* **37** (12):2499-2501.

[26] Park, J., and Shin, H.D. (1997) Experimental investigation of the developing process of an unsteady diffusion flame. *Comb. Flame* **110**:67-77.

[27] Silver, J.A. (1992) Frequency modulation Spectroscopy for trace species detection: theory and comparison among experimental methods. *Appl. Opt.* **31**:707-717.

[28] Silver, J.A., and Kane, D.J. (1999) Diode laser measurements of concentration and temperature in microgravity combustion. *Meas. Sci. Technol.* **10**:845-852.

[29] Silver, J.A., Kane, D.J., and Greenberg, P.S. (1995) Quantitative species measurements in microgravity flames with near-ir diode lasers. *Appl. Opt.* **34**:2787-2801.

[30] Verzicco, R., and Orlandi, P. (1995) Mixedness in the formation of a vortex ring. *Phys. Fluids* **7** (6):1513-1515.

[31] Wang, J., Maiorov, M., Baer, D.S., Garbuzov, D.Z., Connolly, J.C., and Hanson, R.K. (2000) In situ combustion measurements of CO with diode-laser absorption near 2.3 μm. *Appl. Opt.* **39** (30):5579-5589.

[32] You, Y.H., Lee, D.K., and Shin, H.D. (1998) Visual investigation of a vortex ring interacting with a nonpremixed flame. *Combust. Sci. Tech.* **139**:365-383.